Research Journal of Applied Sciences, Engineering and Technology 14(3): 112-118, 2017
DOI:10.19026/rjaset.14.4153
ISSN: 2040-7459; e-ISSN: 2040-7467

Submitted: November 21, 2016 Accepted: February 13, 2017 Published: March 15, 2017

Research Article

Modeling and Simulation of Double Gate Field Plate $In_{0.2}Ga_{0.8}$ As/$Al_{0.3}$ $Ga_{0.7}$ as HEMT using Gaussian Process Regression for Sensor Application

Yousfi Abderrahim, Dibi Zohir, Guermoui Mawloud and Aissi Salim
Department of Electronics, Advanced Electronic Laboratory (LEA), Batna-2-University, Avenue Mohamed El-Hadi Boukhlouf, 05000, Batna, Algeria

Abstract: We propose a new approach for modeling a High Electron Mobility Transistor (HEMT) using that of Gaussian Process Regression one (GPR), to improve the current-voltage characteristics of HEMT transistor for using in electronic and biological domain or any other domain that needs it. The study and development of a new Atlas Silvaco device are taking into account the impact of several geometric and electric parameters; we focus on the electrical performances of the double gate field plate $In_{0.2}Ga_{0.8}As/Al_{0.3}Ga_{0.7}As$ HEMT including double hetero-structure; we compare the numerical simulation using 2D Atlas Silvaco simulator with the extracted experimental results. Then we validate our model by GPR approach. The GPR approach opens promising opportunities for devices modeling without knowing too much the device physics properties. The obtained results give better performances which lead to fabricate devices with better electrical properties for promoting further investigation.

Keywords: 2D Atlas Silvaco, double hetero structure, GPR, HEMT

INTRODUCTION

A few years ago HEMTs based on GaAs attracted the attention of researchers in several domains due to its variety of applications such as: military communications, radar, intelligence applications and sensors (DNA and image) (Wang *et al*., 2015; Lai *et al*., 2007). According to the increase in its transfer characteristics drain-source current I_{ds} functions of the drain-source voltage V_{ds} consumption are of primary importance in designs and preferred transistor technology for demanding millimeter-wave electronics where power gain, signal to noise ratio (Chen *et al*., 2000). Many Machine Learning algorithms have been proposed to simulate and modeling the behavior designs by knowing and exploiting only the geometric parameters. Several articles treated with different category of regression methods and obtain good results, which followed by a certain parameters like: CorrCoef, RMSE, RRMSE and MABE2 as they did in the following articles: organic field effect transistor (OFET) using artificial neural networks (MLP) (Benacer and Dibi, 2014), HEMT Transistor Noise modeling using generalized radial basis function (Hayati *et al*., 2008), HEMTs based on artificial neural networks (Hayati and Akhlaghi, 2013), Improving Ion-Sensitive Field-Effect Transistor Selectivity with Back propagation Neural Network (MLP) (Abdullah *et al*., 2010), Double gate MOSFET modeling based on adaptive neuro-fuzzy inference system for nanoscale circuit simulation (ANFIS) (Hayati *et al*., 2010), Modeling and Design of Inverter Threshold Quantization Based Current Comparator using Artificial Neural Networks (MLP) (Bhatia *et al*., 2016), RBF Network Optimization of Complex Microwave Systems Represented by Small FDTD Modeling Data Sets (Murphy and Yakovlev, 2006), Overview of Microwave Device Modeling Techniques Based on Machine Learning (SVM, SVR, GA, ANN) (Zhao *et al*., 2013).

In the present study, we need to design a minimize model based on a numerical study platform of double gate field plat $In_{0.2}Ga_{0.8}As/Al_{0.3}Ga_{0.7}As$ HEMT including double hetero-structure. Our numerical modeling helps to downsizing the gate, channel length, channel width and double hetero structure which lead to the increase of the drain-source current that is proportional reversed with the gate-source voltage. Minimization benefits are very suitable for DNA and image sensor which are used in nanometric area accompanied with attractive short time response.

The aim of this study is to propose a new modeling method based on numerical simulation and the GPR approach of double gate field plat

Corresponding Author: Yousfi Abderrahim, Department of Electronics, Advanced Electronic Laboratory (LEA), Batna-2-University, Avenue Mohamed El-Hadi Boukhlouf, 05000, Batna, Algeria, Tel.: (213) 0667319749; Fax: (0)33 86 61 80

$In_{0.2}Ga_{0.8}As/Al_{0.3}Ga_{0.7}As$ HEMT including double hetero-structure in order to improve the drain-source current, then high sensitivity and fast response time are all achieved.

In this context, the numerical simulation using 2-D Atlas Silvaco (Atlas user's Manual, 2012) of the proposed and conventional designs of $In_{0.2}$ $Ga_{0.8}$ $As/Al_{0.3}Ga_{0.7}As$ HEMT is presented where the proposed design shows high performances in terms of transfer characteristics over the experimental results obtained by Wang *et al*. (2015). The effectiveness of the proposed design is proved by using GPR approach.

This study is organized as follows. First, we show the numerical simulation via Atlas Silvaco simulator of double gate field plate $In_{0.2}Ga_{0.8}As/Al_{0.3}Ga_{0.7}As$ HEMT including double hetero-structure. After that, we make a comparison between the numerical results and the extracted experimental results. Finally, we validate our model by the use of (GPR) approach.

MODELING METHODOLOGY

This study took three years ago, simulated at the university of Batna-2-Algeria, through 2D Atlas Silvaco and Matlab simulator. The GPR approach used to modulated and prove the transfer characteristic current-voltage of HEMT transistor.

The modelofdouble gate field plate $In_{0.2}Ga_{0.8}As/Al_{0.3}Ga_{0.7}As$ HEMT including double hetero-structure used in DNA sensor as we mentioned (Wang *et al*., 2015). For us, we want to employ HEMT in image sensor for the next work based on this model to get better one.

In the following section, we study the numerical modeling of the geometrical parameters needed for the performance enhancement of double gate field plate $In_{0.2}Ga_{0.8}As/Al_{0.3}Ga_{0.7}As$ HEMT including double hetero-structure using 2D Atlas Silvaco and Gaussian process regression approach.

Numerical simulation: The structure of double gate field plate $In_{0.2}Ga_{0.8}As/Al_{0.3}Ga_{0.7}As$ HEMT including double hetero-structure is modulated and simulated via Atlas 2D Silvaco. Our contribution will be the insertion of a second gate field plate, second hetero-structure, the two regions of the drain and source are chosen as separate areas. The cross section schematic device of double gate field plat $In_{0.2}Ga_{0.8}As/Al_{0.3}Ga_{0.7}As$ HEMT including double hetero-structure is shown in Fig. 1. The device structure consists of a symmetrical design from the top gate to channel and bottom gate to channel, the drain and source are heavily doped to insure the best control of the channel current via the double gate field plate voltage. Source and drain are two regions of GaAs doped of $3\times10^{18}cm^{-3}$. Table 1 describes the dimensions of our model.

The mesh uses in the interface of hetero-structure $In_{0.2}Ga_{0.8}As/Al_{0.3}Ga_{0.7}As$ are carefully chosen as very smaller spacing regions with specific values. The 2DEG (two Dimensional Electron Gaz) appears between the hetero-structure $In_{0.2}Ga_{0.8}As/Al_{0.3}Ga_{0.7}As$ is insured with silicon δ-doping layer (Lin *et al*., 2007).

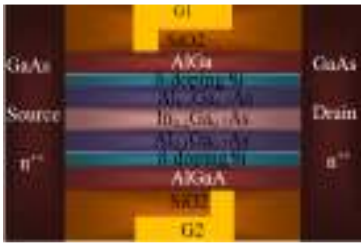

Fig. 1: Structure of double gate field plate $In_{0.2}$ $Ga_{0.8}$ $As/Al_{0.3}Ga_{0.7}As$ HEMT including double hetero-structure

Table 1: The dimensions of a double gate field plate $In_{0.2}$ $Ga_{0.8}$ $As/Al_{0.3}Ga_{0.7}As$ HEMT including double hetero-structure

	Device dimension	
Layer	Doping (cm^{-3})	Thickness (nm)
Channel $In_{0.2}Ga_{0.8}As$	Undoped	15
Spacer $Al_{0.3}Ga_{07}As$	Undoped	4
Si δ-doping	$2,8\times10^{18}cm^{-3}$	4
Barrier $Al_{0.3}Ga_{07}As$	Undoped	15

The present model of double gate field plat $In_{0.2}Ga_{0.8}As/Al_{0.3}Ga_{0.7}As$ HEMT including double hetero-structure offers a high drain-source current with a lower applied voltage drain to source accompanied with high electron mobility, the characteristic current-voltage (I-V) offers good performances for sensor applications as DNA and image.

Theory of Gaussian Process Regression (GPR): GPR has become increasingly a powerful statistical tool for data-driven modeling. GPR models are a Bayesian non parametric approach that can be applied to solve classification and regression supervised ML problems. It has been applied to response surface modeling (Yuan *et al*., 2008), system identification (Chan *et al*., 2013), calibration of spectroscopic analyzers (Ni *et al*., 2014; Wang *et al*., 2011) and ensemble learning (Liu and Gao, 2015).

The main idea of GPR modeling is to place a prior directly on the space of functions. The combination of the prior and the data leads to the posterior distribution over functions. We focus on using the GPR approach for modeling the DGSR over the semi arid area.

We consider a regression of x group which containing d variables. In machine-learning approach the main objective is to learn the functional relationship between the inputs of d-dimensional $x \in R^d$ and the output variable *y*:

$$y = f(x) \tag{1}$$

Hence R and f(x) denote respectively the real space and the unknown function. The unknown function *f* can

be approximated by the following linear combination of the basic function:

$$\hat{f}(x,w)=\sum_{j=1}^{M}W_j\phi_j(x) \tag{2}$$

$\{\phi_j(x)\}_{j=1}^{M}$ represent a set of basis function which could be linear or nonlinear and $w=[w_1,...,w_M]^T$ is the unknown vector for M basis function of the unknown function f .

$$y=\sum_{j=1}^{M}W_j\phi_j(x)+\varepsilon \tag{3}$$

In Eq. (3) ε represents the error term. In general wide range of linear and nonlinear regression models uses a set of training data $D=\{X,Y\}_{i=1}^{N}$ of N observation to estimate the unknown weights W and the basis function $\Phi_j(x)$ can be seen as a transformation of the data from the original space into high dimensional space which is not the case in GPR models, as will be shown below.

In their study, Rasmussen and Williams (2006) mentioned that the basic block of GPR is GP that assumes Gaussian priors for function values specified which is specified by its second order statistics:

$$f(x)\approx GP(m(x),k(x,\bar{x})) \tag{4}$$

where, M(x), k(x, $\bar{x}$) represent the mean and the covariance function of the unknown function f. By definition GP is a finite set of random variables with joint Gaussian distribution (Sun *et al*., 2014). Under GP, the prior distribution of f is Gaussian:

$$p\langle f\,|\,X,\theta\rangle\approx N(0,K) \tag{5}$$

The mean of f is assumed to be zero and the N × N matrix K is a covariance matrix of function f with its hyper parameters denoted by θ.

If the error term ε in Eq. (3) is independent and identically Gaussian distributed, the likelihood function of the training target is also Gaussian:

$$p\left\langle y\,\middle|\,f,\sigma^2\right\rangle\approx N(f,\sigma^2) \tag{6}$$

where, σ^2 and I denote the variance of model error and identity matrix respectively. Then the posterior distribution of the function f can be obtained by applying the Bayes' rule:

$$p\left\langle f\,\middle|\,y,X,\theta,\sigma^2\right\rangle=\frac{p\left\langle y\,\middle|\,f,\sigma^2\right\rangle p\langle f\,|\,X,\theta\rangle}{p\left\langle y\,\middle|\,X,\theta,\sigma^2\right\rangle} \tag{7}$$

Note that the posterior distribution of the function f is also Gaussian, since both the prior and likelihood function is Gaussian. From Rasmussen and Williams (2006) the mean and covariance of posterior distribution are:

$$\mu=K^T(K+\sigma^2I)^{-1}y \tag{8}$$

$$\Sigma=K-K^T(K+\sigma^2I)^{-1}y \tag{9}$$

We note that the covariance function $K(..,.)$ is referred to as Kernel function in machine learning. In GPR literature are commonly used kernel functions including squared exponential or Gaussian kernel (Rasmussen and Williams, 2006):

$$K\langle x,\bar{x}\,|\,\theta\rangle=\sigma_f^2\exp(-\frac{r^2}{2I^2}),\theta=\{\alpha,I,\sigma_f^2\} \tag{10}$$

And the matern family of covariance function is:

$$K\langle x,\bar{x}\,|\,\theta\rangle=\sigma_f^2\frac{2^{1-\upsilon}}{r(\upsilon)}(\frac{\sqrt{2\upsilon}\,r}{I})^{\upsilon}K_{\upsilon}(\frac{\sqrt{2\upsilon}\,r}{I}),\quad\theta=\{\upsilon,I,\sigma_f^2\} \tag{11}$$

In Eq. (10) and (11) the term r = |x - $\bar{x}$| denote the Euclidean distance between two points and θ represent the hyper parameters associated with each covariance function. The variance noise σ^2 is a set of additional parameters that are determined during the training phase. The marginal probability distribution can be estimated by integration over the unknown function f:

$$p\langle y\,|\,x\rangle=\int p\left\langle y\,\middle|\,f,\sigma^2\right\rangle p\langle f\,|\,x,\theta\rangle df \tag{12}$$

The log marginal likelihood is obtained:

$$\log p\langle y\,|\,x\rangle\propto-\frac{1}{2}y^T(K+\sigma^2I)^{-1}\quad y-\frac{1}{2}\log\left|K+\sigma^2I\right|-\frac{N}{2}\log(2\pi) \tag{13}$$

The unknown parameters (θ, σ^2) can be estimated from Eq. (13) using gradient based algorithm. Since the posterior of f is determined through training data, we can evaluate the predictive distribution of any test data x_* and we obtain the function conditioned on training results:

$$p\left\langle f_*\,\middle|\,x_*,y,X,\theta,\sigma^2\right\rangle \tag{14}$$

From Liu and Gao (2015) which could be shown that the predictive distribution of Eq. (14) is Gaussian with mean m and variance υ^2 given by:

$$m(x_*) = \phi(x_*)^T \mu = K_*^T (K + \sigma^2 I)^{-1} y \quad (15)$$

$$\sigma^2(x_*) = \phi(x_*)^T \Sigma \phi(x_*) = K_{**} - K_*^T (K + \sigma^2 I)^{-1} K \quad (16)$$

$$K_* = [K(x_*, x_1) ..... K(x_*, x_N)]^T, K_{**} = K(K_* + x_*)$$

where, μ and Σ are the posterior mean and variance of f. The prior mean was assumed to zeros and the kernel function used in the present work is squared exponential.

RESULTS AND DISCUSSION

To verify the effectiveness of the proposed design, the 2D Atlas Silvaco (ATLAS User's Manual, 2012) is used to simulate the transfer characteristic $I(V)$.

In order to validate the accuracy of the designed device, the obtained results are implemented in Gaussian Process Regression algorithm (GPR) as data base input.

A close matching is achieved between the extracted experimental results (Wang *et al*., 2015) and its numerical simulation which is well done in this study as shown in Fig. 2, the transfer characteristics I_{ds} versus of V_{ds} with different values of V_{gs} which is selected

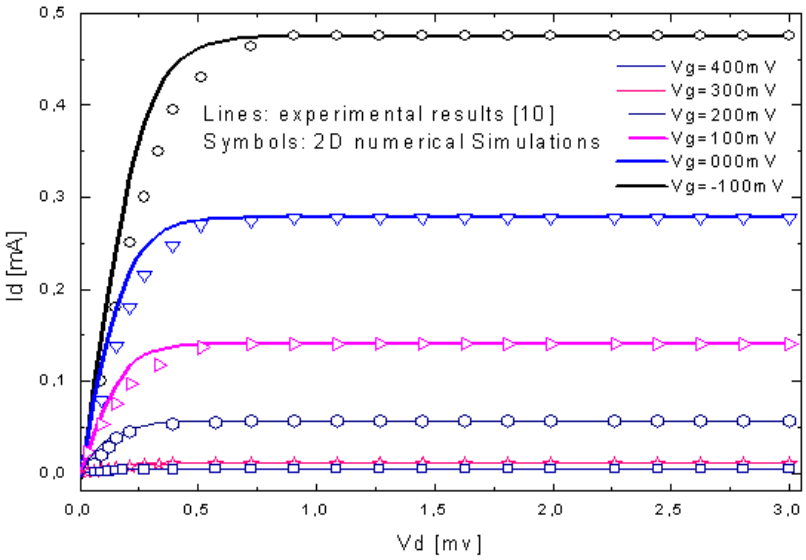

Fig. 2: Numerical and experimental results for the conventional AlGaAs/InGaAs high electron mobility transistors (Wang *et al*., 2015)

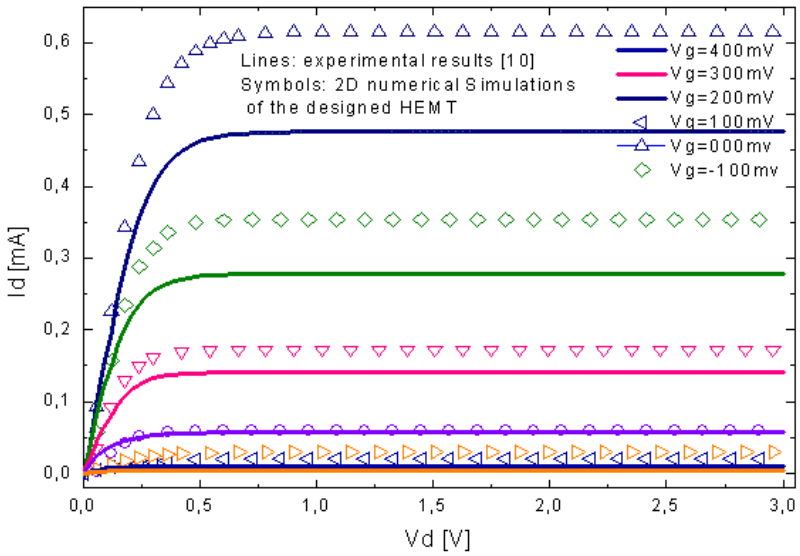

Fig. 3: Comparison between numerical results of double gate field plate $In_{0.2}Ga_{0.8}As/Al_{0.3}Ga_{0.7}As$ HEMT including double hetero-structure and experimental results of AlGaAs/InGaAs HEMT (Wang *et al*., 2015)

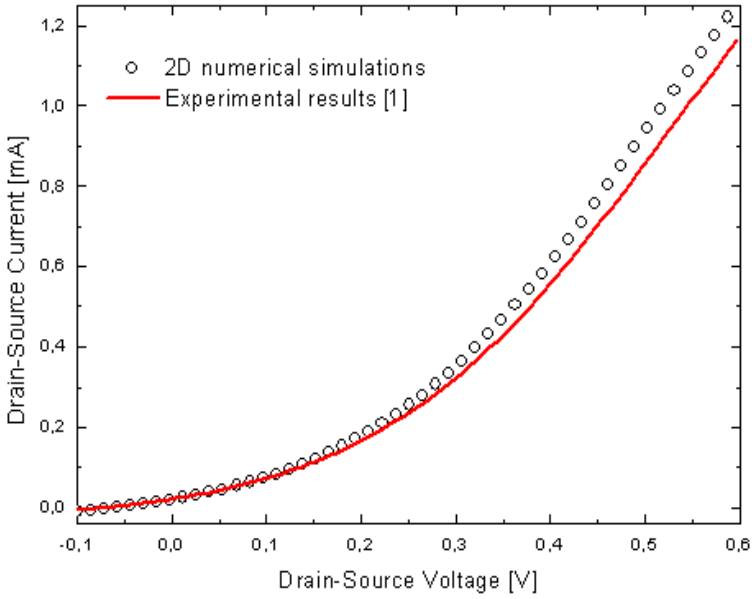

Fig. 4: Comparison between numerical results of the designed HEMT and experimental results for I_{ds}-V_{gs} characteristic

between -100 *mV* to 400 *mV*, V_{ds} range varies up from 0 to 3 *mV* and the output drain current ranges from 0 to 0.48 *mA*. A high drain current is observed when the gate voltage minimized as seen in Fig. 2. The good agreement between the conventional design (Wang *et al*., 2015) and our numerical simulation is due to the accurate modeling using 2D Atlas Silvaco simulator.

In Fig. 3, the transfer characteristics of the current-voltage of the proposed design are plotted and a high drain current is observed when the gate voltage gets lower values as seen in Fig. 3. The obtained results of the proposed design shows a higher drain current (I_{ds} = 0.61mA) over the conventional design (experimental data) (I_{ds} = 0.48mA). This enhancement is due to the decisive impact of the geometrical parameters which has an important effect on the drain current and, therefore, the electrical performances of the HEMT.

Figure 4 illustrates the variation of drain current functions of gate voltage. The proposed design shows upper drain current over the conventional design; according to this Fig. 4, the model also offers high performances in terms of downscaling device and low power consumption.

In this section of comparison, we obtain a good agreement that is shown in Fig. 3 and 4 which give a higher values of current for double gate field plate $In_{0.2}Ga_{0.8}As/Al_{0.3}Ga_{0.7}As$ HEMT including double hetero-structure versus the model of Wang *et al*. (2015).

MODEL VALIDATION METHODS

In this study, the performance of GPR modeling for the drain-source current is evaluated by comparing the estimated values with the measured values using different statistical indexes such as Mean Absolute Bias Error (MABE), Root Mean Square Error (RMSE), Relative Root MeanSquare Error (RRMSE), Determination Coefficient (R^2) and Correlation Coefficient (r).The MABE gives the mean absolute values of bias error obtained by:

$$MABE = \frac{1}{n}\sum_{i=1}^{n}\left|H - \overline{H}\right| \tag{17}$$

where, $\overline{H}$ and H are respectively the estimated and the measured values. The RMSE represents the difference between the predicted values estimated by the model and the measured values. In fact, RMSE identifies the model's accuracy calculated by:

$$RMSE = \sqrt{\frac{1}{n}\sum_{i=1}^{n}(H - \overline{H})^2} \tag{18}$$

The RRMSE is calculated by dividing the RMSE to the average of measured data as:

$$RRMSE = \frac{\sqrt{\frac{1}{n}\sum_{i=1}^{n}(H - \overline{H})^2}}{\frac{1}{n}\sum_{i=1}^{n}H} \tag{19}$$

The ranges of RRMSE define the model performance as:

Excellent if: RMSE $\prec$ 10%
Good if: 10% $\prec$ RMSE $\prec$ 20%
Fair if: 20% $\prec$ RMSE $\prec$ 30%
Poor if: RMSE $\succ$ 30%

Table 2: Data ranges for inputs used in this simulation

Coefficient input	Value	
	Min	Max
V_{ds}(V)	0.6	-0.1
V_{gs}(mV)	400	-100
L (μm)	80	60
Thickness (nm)	17	12
Output		
I_{ds}(mA)	0	0.061

Table 3: Coefficients and values of GPR approach

Coefficient	Value
CorrCoef	0.9998
RMSE	0.0081
RRMSE	4.4045
MABE2	0.0069

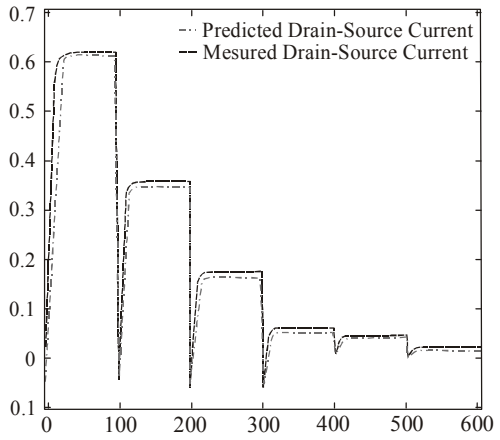

Fig. 5: Illustration of predicted and measured Drain-Source current via GPR

The *r* indicates the strength of a linear relationship between the measured and predicted values is calculated as follows:

$$r = \frac{\sum_{i=1}^{n}(H_p - \overline{H}_p)(H_M - \overline{H}_M)}{\sqrt{\sum_{i=1}^{n}(H_p - \overline{H}_p).\sum_{i=1}^{n}(H_M - \overline{H}_M)}} \quad (20)$$

The data range of the maximum and minimum values for the transfer characteristic and the data of GPR modeling are resumed in Table 2.

Figure 5 shows current-voltage characteristic of double gate field plat $In_{0.2}Ga_{0.8}As/Al_{0.3}Ga_{0.7}As$ HEMT, a close matching of the predicted and the measured drain-source current along the channel. Figure 6 presents the comparison between the numerical results and the predicted results using the GPR approach, good agreement illustrated between the two lines.

Table 3 contains the values of regression coefficients for the present approach which is done by GPR.

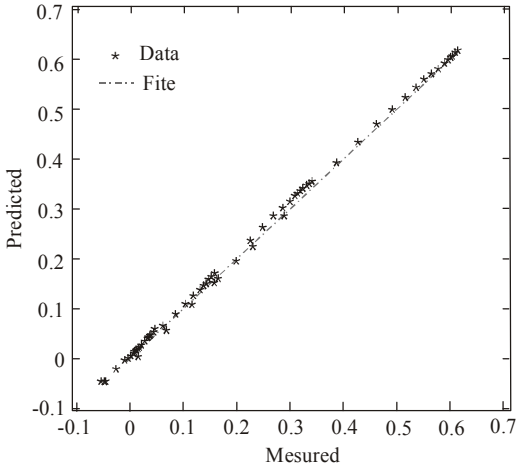

Fig. 6: Comparison between numerical and predicted results using GPR

CONCLUSION

The numerical modulation of double gate field plate $In_{0.2}Ga_{0.8}As/Al_{0.3}Ga_{0.7}As$ HEMT including double hetero-structure using 2D Atlas Silvaco is presented. The effectiveness of the proposed design is approved by using the Gaussian Process Regression approach (GPR). The obtained values show high electrical performances and low cost fabrication over the conventional design. The proposed methodology opens promising opportunities for devices modeling without sufficient knowledge of the device physics properties.

REFERENCES

Abdullah, W.F.H., M. Othman, M.A.M. Ali and M.S. Islam, 2010. Improving ion-sensitive field-effect transistor selectivity with backpropagation neural network. WSEAS T. Circuit. Syst., 9(11): 700-712.

ATLAS User's Manual, 2012. Device simulation software, 2012. Silvaco International, Santa Clara, CA.

Benacer, I. and Z. Dibi, 2014. Modeling and simulation of organic field effect transistor (OFET) using artificial neural networks. Int. J. Adv. Sci. Technol., 66: 79-88.

Bhatia, V., N. Pandey and A. Bhattacharyya, 2016. Modelling and design of inverter threshold quantization based current comparator using artificial neural networks. Int. J. Elect. Comput. Eng., 6(1): 320-329.

Chan, L.L.T., Y. Liu and J. Chen, 2013. Nonlinear system identification with selective recursive Gaussian process models. Ind. Eng. Chem. Res., 52(51): 18276-18286.

Chen, Y.C., R. Lai, D.L. Ingram, T. Block, M. Wojtowicz, P.H. Liu, H.C. Yen, A. Oki, D.C. Streit and K. Yano, 2000. Highly efficient high power InP HEMT amplifiers for high frequency applications. Proceeding of the 58th IEEE DRC Devices Research Conference, pp: 139-140.

Hayati, M. and B. Akhlaghi, 2013. An extraction technique for small signal intrinsic parameters of HEMTs based on artificial neural networks. AEU Int. J. Electron. Commun., 67(2): 123-129.

Hayati, M., A. Shamkhani, A. Rezaei and M. Seifi, 2008. HEMT Transistor Noise modeling using generalized radial basis function. Proceeding of the IEEE International Conference on Semiconductor Electronics, pp: 509-513.

Hayati, M., M. Seifi and A. Rezaei, 2010. Double gate MOSFET modeling based on adaptive neuro-fuzzy inference system for nanoscale circuit simulation. ETRI J., 32(4): 530-539.

Lai, R., X.B. Mei, W.R. Deal, W. Yoshida, Y.M. Kim, P.H. Liu, J. Lee, J. Uyeda, V. Radisic, M. Lange, T. Gaier, L. Samoska and A. Fung, 2007. Sub 50 nm InP HEMT device with fmax greater than 1 THz. Proceeding of the IEEE International Electron Devices Meeting, pp: 609-611.

Lin, J.C., P.Y. Yang and W.C. Tsai, 2007. Simulation and analysis of metamorphic high electron mobility transistors. Microelectron. J., 38(2): 251-254.

Liu, Y. and Z. Gao, 2015. Real-time property prediction for an industrial rubber-mixing process with probabilistic ensemble Gaussian Process Regression models. J. Appl. Polym. Sci., 132(6): 1905-1913.

Murphy, E.K. and V.V. Yakovlev, 2006. RBF network optimization of complex microwave systems represented by small FDTD modeling data sets. IEEE T. Microw. Theory, 54(7): 3069-3083.

Ni, W., L. Nørgaard and M. Mørup, 2014. Non-linear calibration models for near infrared spectroscopy. Anal. Chim. Acta, 813: 1-14.

Rasmussen, C.E. and C.K.I. Williams, 2006. Gaussian Processes for Machine Learning. Adaptive Computation and Machine Learning. MIT Press, Cambridge, Mass, 17: 48.

Sun, A.Y., D. Wang and X. Xu, 2014. Monthly streamflow forecasting using Gaussian process regression. J. Hydrol., 511: 72-81.

Wang, C., Y. Zhang, M. Guan, L. Cui, K. Ding, B. Zhang, Z. Lin, F. Huang and Y. Zeng, 2015. Specific detection of mercury(II) irons using AlGaAs/InGaAs high electron mobility transistors. J. Cryst. Growth, 425: 381-384.

Wang, K., T. Chen and R. Lau, 2011. Bagging for robust non-linear multivariate calibration of spectroscopy. Chemometr. Intell. Lab., 105(1): 1-6.

Yuan, J., K.S. Wang, T. Yu and M.L. Fang, 2008. Reliable multi-objective optimization of high-speed WEDM process based on Gaussian process regression. Int. J. Mach. Tool. Manu., 48(1): 47-60.

Zhao, Z., Y. Qu, Y. Zhang and X. Shen, 2013. Overview of microwave device modeling techniques based on machine learning. Int. J. Adv. Comput. Technol., 5(9): 299-306.